

Action-Sufficient Goal Representations

Jinu Hyeon ^{* 1} Woobin Park ^{* 1} Hongjoon Ahn ^{* 1} Taesup Moon ^{1 2 3}

Abstract

Hierarchical policies in offline goal-conditioned reinforcement learning (GCRL) addresses long-horizon tasks by decomposing control into high-level subgoal planning and low-level action execution. A critical design choice in such architectures is the goal representation—the compressed encoding of goals that serves as the interface between these levels. Existing approaches commonly derive goal representations while learning value functions, implicitly assuming that preserving information sufficient for value estimation is adequate for optimal control. We show that this assumption can fail, even when the value estimation is exact, as such representations may collapse goal states that need to be differentiated for action learning. To address this, we introduce an information-theoretic framework that defines *action sufficiency*, a condition on goal representations necessary for optimal action selection. We prove that value sufficiency does not imply action sufficiency and empirically verify that the latter is more strongly associated with control success in a discrete environment. We further demonstrate that standard log-loss training of low-level policies naturally induces action-sufficient representations. Our experimental results a popular benchmark demonstrate that our actor-derived representations consistently outperform representations learned via value estimation.

1. Introduction

The primary advantage of offline goal-conditioned reinforcement learning (GCRL) lies in its ability to extract diverse and complex skills from pre-collected datasets without further environment interaction (Park et al., 2025b; Chane-Sane

et al., 2021; Eysenbach et al., 2022; Liu et al., 2022; Ma et al., 2022). However, the efficacy of this paradigm fundamentally depends on how state and goal information are encoded into a shared representation space to bridge the gap between observed data and target behaviors. This becomes even more critical in long-horizon tasks, where hierarchical frameworks are often employed. In such systems, a high-level planner provides subgoals to a low-level controller, and the effectiveness of this hierarchy hinges on the quality of the goal representation space used to communicate these subgoals.

A prominent example of this approach is HIQL (Park et al., 2023), which learns goal representations directly through the value learning objective and utilizes them to facilitate high-level planning. While HIQL has demonstrated significant empirical success in complex, long-horizon environments, a systematic understanding of why value-centric representations work—and specifically how they relate to the downstream low-level policy—remains incomplete. While Park et al. (2025d) recently provided a rigorous interpretation from the standpoint of value estimation, a critical gap persists: the lack of a policy-oriented analytical framework. Our work challenges the implicit assumption that features optimized for learning value functions naturally facilitate policy learning. By introducing the concept of action sufficiency, we provide a novel information-theoretic analysis showing that representations derived solely from value-based objectives often fail to capture the essential information required for robust policy derivation in offline settings.

To investigate the potential limitations of these established approaches, we first conduct empirical evaluations in the cube task from OGBench (Park et al., 2025a), specifically measuring the performance of low-level policies. Our results reveal a significant failure mode: agents utilizing value-centric representations exhibit markedly low success rates, suggesting that such features may lack critical information for effective action selection. To explain this phenomenon, we introduce the formal concepts of value sufficiency and action sufficiency, defined by whether a goal representation preserves necessary information for accurate value prediction or optimal policy derivation, respectively.

Using these definitions, we theoretically demonstrate that

^{*} Equal Contribution

¹Department of Electrical and Computer Engineering (ECE), Seoul National University ²Interdisciplinary Program in Artificial Intelligence (IPAI), Seoul National University ³ASRI / INMC, Seoul National University. Correspondence to: Taesup Moon <tsmoon@snu.ac.kr>.

value sufficiency does not inherently guarantee action sufficiency of goal representations. We show that representations optimized solely to reflect value magnitudes can discard relative action-relevant nuances, leading to a fundamental disconnect between value accuracy and policy success. This theoretical finding is further validated through a series of toy examples and the cube task in OGBench (Park et al., 2025a), where we illustrate that there are plenty of cases that value-sufficient features fail in practice. Consequently, we argue that to learn truly action-sufficient features, the representation learning process should be directly integrated with the actor’s objective, ensuring the latent space preserves the essential information-theoretic requirements for optimal control.

2. Preliminary

Problem Setting. Goal-conditioned reinforcement learning (GCRL) is formulated as a Markov Decision Process (MDP) defined by the tuple $(\mathcal{S}, \mathcal{A}, \mathcal{G}, r, \gamma, p_0, p)$. Here, \mathcal{S} denotes the state space, \mathcal{A} the action space, and \mathcal{G} the goal space. The reward function $r(s, g)$ is conditioned on both the current state $s \in \mathcal{S}$ and the goal $g \in \mathcal{G}$, $\gamma \in (0, 1)$ is the discount factor, $p_0(\cdot)$ is the initial state distribution, and $p(\cdot | s, a)$ represents the environment transition dynamics. We denote by $V(s, g)$ the goal-conditioned state-value function at state s with respect to goal g . Throughout this work, we assume that the goal space coincides with the state space, *i.e.*, $\mathcal{G} = \mathcal{S}$.

In the offline setting, the agent is given access to a fixed dataset \mathcal{D} consisting of trajectories $\tau = (s_0, a_0, s_1, \dots, s_T)$, collected by an unknown behavior policy μ . The objective is to learn a goal-conditioned policy $\pi(a | s, g)$ that maximizes the expected discounted return

$$\mathcal{J}(\pi) = \mathbb{E}_{\tau \sim p^\pi(\tau), g \sim p(g)} \left[\sum_{t=0}^T \gamma^t r(s_t, g) \right], \quad (1)$$

where the trajectory distribution induced by π is given by $p^\pi(\tau) = p_0(s_0) \prod_{t=0}^{T-1} p(s_{t+1} | s_t, a_t) \pi(a_t | s_t, g)$, and $p(g)$ denotes a distribution over goals.

Hierarchical Policies in Goal-Conditioned RL. To solve long-horizon tasks, hierarchical reinforcement learning (HRL) decouples the decision-making process into two levels: a high-level planner and a low-level controller. A representative framework, HIQL (Park et al., 2023), builds this hierarchy using value functions learned via Implicit Q-Learning (IQL) (Kostrikov et al., 2022). The high-level policy $\pi^h(s_{t+k} | s_t, g)$ proposes a k -step subgoal to guide progress toward a distant goal g , while the low-level policy $\pi^\ell(a_t | s_t, s_{t+k})$ generates primitive actions to reach the proposed subgoal. Both policies are typically extracted using advantage-weighted regression (AWR) (Peng et al.,

2019), and the exact formula is described in Appendix A (15) and (14).

Goal Representation Learning. A critical component of this hierarchical framework is how subgoals are represented and communicated between levels. In practice, HIQL learns a value-based goal representation $\phi_V(s, g)$ —by concatenating state and goal features—as part of the value function training process. Specifically, the value function is parameterized as $V(s, g) = V_\theta(s, \phi(s, g))$, where the representation ϕ is optimized to minimize the value estimation error via temporal-difference (TD) learning. In HIQL, once the value-based representation is learned, this same representation $\phi_V(s_t, s_{t+k})$ is utilized as a proxy for the subgoal s_{t+k} when training both π^h and π^ℓ (*i.e.*, $\pi^h(\phi_V(s_t, s_{t+k}) | s_t, g)$ and $\pi^\ell(a_t | s_t, \phi_V(s_t, s_{t+k}))$). Note that during training the both policy π^h and π^ℓ , we freeze the goal representation encoder ϕ_V to fully utilize the goal representation learned from training the value function. While this value-centric representation learning has shown empirical success, it remains unclear whether a feature space optimized for value prediction is inherently suitable for policy extraction. In this paper, we deeply analyze the role of $\phi_V(s_t, s_{t+k})$ in policy learning and demonstrate that representations learned solely from value-based objectives can lead to significant failure modes in low-level control.

3. Motivation

3.1. Are Value-based Goal Representations Sufficient for Control?

Hierarchical methods for GCRL typically utilize a latent goal encoder from the value function to handle high-dimensional goal spaces (Park et al., 2023). This practice assumes that representations optimized for **predicting values** are sufficient for **action prediction** (Park et al., 2025d). In this section, we investigate this assumption through an experiment inspired by Ahn et al. (2025), designed to isolate the controllability of the low-level policy.

Oracle Subgoal Evaluation. To isolate low-level controllability from high-level planning errors, we replace predicted subgoals with oracle planner provided in OGBench (Park et al., 2025a). Specifically, given an optimal trajectory τ^* , the policy conditions on the exact oracle subgoal s_{t+k} . In this setting, we compare the original HIQL **value-based goal representation** $\phi_V(s, g)$ learned via optimizing the value objective against the **actor-based goal representation** $\phi_A(s, g)$, which is learned via optimizing the AWR loss (15) with the low-level policy $\pi^\ell(a_t | s_t, \phi_A(s_t, g))$ ¹. Note that all the low-level policies using either ϕ_V or ϕ_A are trained with original goal g , not with the short-horizon subgoal s_{t+k} . After training the policy, we give the oracle

¹To make the learned representation be generalizable across various goals, we use g instead of using s_{t+k} .

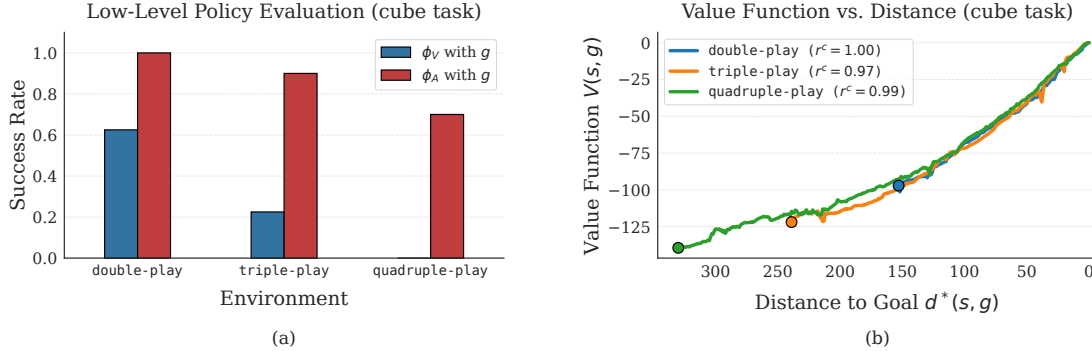


Figure 1. Left: The results of low-level policy evaluation on short-horizon subgoal s_{t+k} from optimal trajectory τ^* . Right: The visualization of value function $V(s, g)$ by varying s from initial state to goal g in τ^* . Note that though the value function effectively captures the discounted temporal distance throughout all environments, the low-level policy equipped with ϕ_V achieves much lower success rate than the counterpart which uses ϕ_A .

subgoal s_{t+k} from the optimal trajectory τ^* to the low-level policy.

The Discrepancy between Value and Control. We measure the goal success rates of the low-level policy conditioned on these oracle subgoal representations. As shown in Figure 1(a), the policy using ϕ_A significantly outperforms the policy using ϕ_V , despite both receiving perfect subgoal information from the oracle. This performance gap indicates that ϕ_V can fail to capture information necessary for action prediction.

Is the Value Function Reliable? One might hypothesize that this failure stems from poor training of the value function itself rather than an inherent limitation of the representation. To investigate this, we measure the *order consistency ratio* $r^c(V)$, a metric proposed by Ahn et al. (2025) to evaluate the reliability of learned value functions:

$$r^c(V) = \frac{1}{T-k+1} \sum_{t=0}^{T-k} \mathbf{1}[V(s_{t+k}, g) > V(s_t, g)].$$

As illustrated in Figure 1(b), the trained value exhibits high order consistency ratio, confirming that the value network successfully learned the temporal structure of the task.

Summary. These findings reveal that representations optimized for value estimation are not optimal for control, even when the value estimates themselves are reliable. This discrepancy suggests that the information required to *evaluate* a state differs from that required to *act* upon it.

3.2. Value Prediction \neq Optimal Control: A 1D Thought Experiment

To illustrate why a value-preserving goal encoder can be structurally ill-suited for control, we analyze a minimal thought experiment on the integer line, adopting the setting from the motivating example in Park et al. (2023).

Setup. Consider a deterministic MDP where $\mathcal{S} = \mathcal{G} = \mathbb{Z}$

and actions $\mathcal{A} = \{+1, -1\}$ shift the state by a . Under the shortest-path reward $r(s, g) = -1[s \neq g]$, the optimal value depends purely on the distance:

$$V^*(s, g) = -\frac{1 - \gamma^{|s-g|}}{1 - \gamma}. \quad (2)$$

Representations. We compare two distinct goal representations²:

$$\phi_{\text{sign}}(s, g) = s - g, \quad (\text{Preserves direction}) \quad (3)$$

$$\phi_{\text{dist}}(s, g) = |s - g|. \quad (\text{Preserves value only}) \quad (4)$$

Note that both representations allow recovering V^* exactly (i.e., V^* is a function of $|s - g|$).

The Conflict. While ϕ_{dist} is perfect for value prediction, it fails for control. Consider a state s and two opposite goals:

- $g^+ = s + 1 \implies a^* = +1$.
- $g^- = s - 1 \implies a^* = -1$.

Here, ϕ_{dist} maps both goals to the same embedding: $\phi_{\text{dist}}(s, g^+) = \phi_{\text{dist}}(s, g^-) = 1$. Consequently, a policy conditioning on ϕ_{dist} receives identical inputs for distinct optimal actions, making optimal control impossible. In contrast, ϕ_{sign} distinguishes these cases (-1 vs $+1$), enabling the policy to solve the task.

Key message. *A representation can retain all information needed to recover the optimal value while still collapsing distinct goals that require different optimal actions.* This motivates analyzing goal encodings through the lens of control, not only value prediction.

4. Optimal Control Policy Estimation and Action Sufficiency

The previous counterexample motivates a fundamental question: *what properties should a goal representation satisfy to support optimal action selection?* We formalize this via the **conditional KL risk**, measuring the divergence between

²We defer the justification for allowing ϕ to depend on (s, g) rather than solely on g to Appendix C.

the optimal policy and a learned predictor restricted to the representation. This risk decomposes into modeling error and representation error, motivating our core definition: a representation is *action-sufficient* if the representation error vanishes, guaranteeing that compression imposes no ceiling on performance.

4.1. Problem Formulation

Let S , G , and A be random variables representing the state, goal, and optimal action, taking values in measurable spaces \mathcal{S} , \mathcal{G} , and \mathcal{A} , with joint law P . We consider a deterministic representation $Z := \phi(S, G)$ for measurable ϕ .

We frame control within a hierarchical architecture. The *high-level policy* π^h proposes a stochastic subgoal $G_{\text{sub}} \in \mathcal{G}$ given (S, G) , inducing a distribution over representations $Z_{\text{sub}} := \phi(S, G_{\text{sub}})$:

$$\pi^h(\cdot | S, G) \in \mathcal{P}(\mathcal{Z}).$$

The *low-level policy* π^ℓ selects actions conditioned on the state and subgoal representation:

$$\pi^\ell(\cdot | S, Z_{\text{sub}}) \in \mathcal{P}(\mathcal{A}).$$

At deployment, the low-level policy conditions on representations predicted by the high-level policy. Since subgoals and final goals share the same space, we use the notation interchangeably hereafter.

4.2. Conditional KL Decomposition

We analyze the controllability of the low-level policy π^ℓ induced by the representation ϕ . To measure the discrepancy between the optimal policy and this predictor, we employ the **conditional KL risk**:

$$\mathcal{R}(\pi^\ell; \phi) = \mathbb{E} [D_{\text{KL}}(P(A|S, G) \| \pi^\ell(A|S, Z))] . \quad (5)$$

Our analysis yields the following decomposition of this risk:

Proposition 4.1 (Conditional KL Risk Decomposition).
The risk $\mathcal{R}(\pi^\ell; \phi)$ decomposes into:

$$\mathcal{R}(\pi^\ell; \phi) = \underbrace{\mathbb{E} [D_{\text{KL}}(P(A|S, Z) \| \pi^\ell(A|S, Z))]}_{\text{Modeling Error}} + \underbrace{I(A; G | S, Z)}_{\text{Representation Error}},$$

where $I(\cdot; \cdot)$ denotes conditional mutual information.

Full proofs and mathematical details are deferred to Appendix D.

4.3. Action Sufficiency

Proposition 4.1 reveals that optimizing π^ℓ serves only to minimize the modeling error, leaving the second term as an irreducible penalty determined solely by the information loss in ϕ . This motivates our core definition of **action sufficiency**:

Definition 4.2 (Action-Sufficient Representation). A representation $Z = \phi(S, G)$ is *action-sufficient* if:

$$\Delta_A := I(A; G | S, Z) = 0.$$

This condition is equivalent to the conditional independence $A \perp G | (S, Z)$, or almost surely matching the posterior laws: $P(\cdot | S, G) = P(\cdot | S, Z)$. Intuitively, action sufficiency implies that Z retains all goal information requisite for optimal action prediction.

This definition is not arbitrary; it arises from the fundamental conditional KL gap incurred when approximating the goal-conditioned action posterior $P(\cdot | S, G)$ using a policy restricted to conditioning on (S, Z) , with Δ_A capturing the resulting irreducible residual. If $\Delta_A > 0$, no policy $\pi^\ell(\cdot | S, Z)$ can drive the risk in Eq. (5) to zero, even with infinite data and perfect optimization.

5. Value Sufficient Representation Is Not Action Sufficient

In the previous section, we established the concept of **action sufficiency** ($\Delta_A = 0$). Here, we investigate why representations trained solely to predict values, which is a common practice in Hierarchical methods for GCRL (Park et al., 2023; Ahn et al., 2025; Park et al., 2025d), often fail to achieve this standard. We provide detailed proofs for the results presented in this section in Appendix E.

5.1. Optimal Goal-Conditioned Value Function and Value Sufficiency

First, we formalize the value-based perspective. With a discount factor $\gamma \in (0, 1]$ and a goal-conditioned reward function $r(s, g)$, the *optimal goal-conditioned value function* is defined as:

$$V^*(s, g) = \sup_{\pi} \mathbb{E} \left[\sum_{t \geq 0} \gamma^t r(S_t, g) \middle| S_0 = s \right]$$

where the supremum is taken over all possible policies. Following the notation convention established in the definition of action sufficiency, we drop the superscript $*$ and treat the value as a random variable $V := V(S, G)$.

Analogous to action sufficiency, we define the value sufficiency of a representation ϕ as follows:

Definition 5.1 (Value-Sufficient Representation). A representation ϕ is said to be *value-sufficient* (with respect to V) if:

$$\Delta_V := I(V; G | S, Z) = 0 \quad (6)$$

Since V is deterministic with respect to (S, G) , value sufficiency is equivalent to stating that V can be expressed as a function of (S, Z) , i.e., there exists a measurable \tilde{v} such that $V = \tilde{v}(S, Z)$.

5.2. Value Sufficiency Does Not Guarantee Action Sufficiency

While value sufficiency ensures accurate value prediction, it does not necessarily guarantee action sufficiency ($\Delta_A = 0$). The following proposition provides an exact decomposition of the action sufficiency gap when a representation is value-sufficient.

Proposition 5.2 (Action Information Decomposition).

If a representation $Z = \phi(S, G)$ is value-sufficient (i.e., $\Delta_V = 0$), then the action sufficiency gap Δ_A decomposes as:

$$\Delta_A = I(A; G | S, V) - I(A; Z | S, V) \quad (7)$$

This proposition reveals a critical insight: Even if Z preserves the optimal value perfectly, it can still be action-insufficient unless it retains *action-discriminative information among goals that share the same value*.

Conditioning on the value V partitions the goal space into *value level sets*, $\{g : V^*(s, g) = v\}$. Within a fixed level set, goals are indistinguishable in terms of the optimal value, yet can require different optimal actions (e.g., goals N steps away in opposite directions). This mismatch is captured by the residual action-relevant goal information $I(A; G | S, V)$, i.e., the action uncertainty that remains even when the scalar value is known.

The extent to which a representation Z resolves this *within-level-set ambiguity* is quantified by $I(A; Z | S, V)$: it measures how much of the residual uncertainty $I(A; G | S, V)$ is explained by Z beyond the value signal. At the extreme, if $I(A; Z | S, V) = 0$, then the action gap reduces to

$$\Delta_A = I(A; G | S, V),$$

meaning that perfect value sufficiency yields no reduction in action-relevant goal information beyond what is already captured by V .

This phenomenon explains the failure observed in the 1D example in Section 3. In that example, there existed distinct goals g^+ and g^- that shared the same optimal value but required different optimal actions. A representation that failed to distinguish these goals (e.g., ϕ_2) resulted in $I(A; Z | S, V) \approx 0$, creating a structural indistinguishability that prevented optimal control.

More generally, in many non-trivial environments, $I(A; G | S, V)$ is strictly positive. Conditioning on the optimal value alone typically does not resolve goal-dependent action ambiguity. We defer a concrete and plausible sufficient condition guaranteeing $I(A; G | S, V) > 0$ to Appendix F.

In the subsequent section, we empirically demonstrate that even in discrete environments, there exist near-worst-case scenarios where a representation achieves near-perfect value reconstruction ($\Delta_V \approx 0$) while capturing almost no distinct

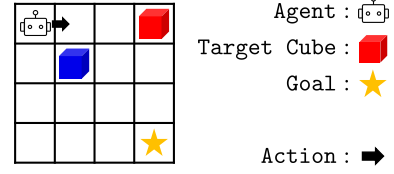


Figure 2. The Discrete Cube environment. This domain mirrors the structure of pick-and-place tasks while allowing for the exact computation of information-theoretic quantities. We use this tractability to rigorously verify that control success depends on preserving action sufficiency rather than value sufficiency.

action information ($I(A; Z | S, V) \approx 0$). This leads to an irreducible control gap where $\Delta_A \approx I(A; G | S, V) > 0$.

Takeaway

We propose **action sufficiency** ($I(A; G | S, Z) = 0$) as a critical prerequisite for optimal control. We prove that **value sufficiency does not imply action sufficiency**: a representation can perfectly predict values yet fail to predict actions.

6. Discrete Cube: Exact Information-Theoretic Analysis

The preceding theoretical analysis established action sufficiency as a fundamental requirement for low-level control. We specifically highlighted that for value-sufficient representations, the conditional mutual information $I(A; Z | S, V)$ emerges as the key quantity governing controllability, representing the information necessary to resolve goal-dependent action ambiguity that persists within value level sets.

To validate our theoretical findings, we introduce the Discrete Cube environment (Figure 2), a tractable grid-world designed for exact information-theoretic analysis.

6.1. Environment Setup: The Discrete Cube

To enable exact information-theoretic analysis, we construct the *Discrete Cube*, a 4×4 grid environment that captures the structural essence of goal-conditioned manipulation in OGBench (Park et al., 2025a) cube tasks. The domain features an agent and two distinct cubes (Red and Blue). The state s consists of the agent’s coordinates, cube positions, and the gripper status (empty or holding a specific cube). The action space \mathcal{A} comprises four directional movements and two manipulation primitives (pick, place).

A goal g specifies a target cube and its desired spatial coordinate. Success is achieved when the target cube reaches the goal position and is released. Crucially, the finite nature of this domain allows us to compute the *exact* optimal value function $V^*(s, g)$ and the optimal policy $P^*(a|s, g)$ via Breadth-First Search (BFS) and derive precise conditional mutual information quantities without estimation error.

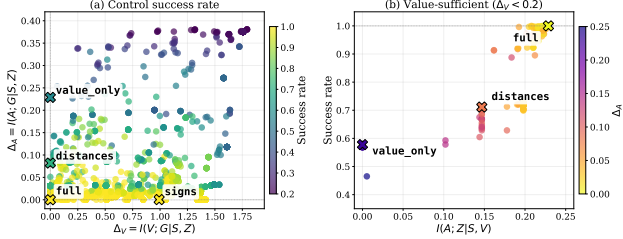


Figure 3. Discrete Cube Result. (a) Control success rate plotted over the (Δ_V, Δ_A) plane for representations ϕ , evaluated using the mixed policy $\pi_\phi(a | s, z)$. (b) For (near-) value-sufficient representations ($\Delta_V < 0.2$), control success rate plotted against $I(A; Z | S, V)$, with points colored by Δ_A .

6.2. Metrics and Control Evaluation

For a fixed representation $Z = \phi(S, G)$, we compute a set of evaluation quantities using the exact environment dynamics: the sufficiency gaps, the within-level-set disambiguation term, and the control success rate.

Sufficiency gaps. We quantify divergence from sufficiency by the conditional mutual informations $\Delta_A = I(A; G | S, Z)$ for control and $\Delta_V = I(V; G | S, Z)$ for value prediction.

Within-level-set disambiguation. We measure how much Z helps distinguish optimal actions among state–goal pairs with identical values via $I(A; Z | S, V)$.

Control success rate. We evaluate the success rate of the mixed policy $\pi_\phi(a | s, z) = \mathbb{E}[P^*(a | s, G) | S = s, Z = z]$, which acts by marginalizing the optimal action distribution over the posterior goal distribution induced by Z .

To systematically investigate the interplay between these metrics, we construct a diverse library of goal representations and randomly sample ϕ from this library. We provide full details on this section, including how we construct the representation library, in Appendix G.

6.3. Results

To facilitate interpretation of the results, we first introduce four representative baselines that anchor the extremes of action and value information: (1) **full**, which preserves the full relative-position information and is both action- and value-sufficient by construction; (2) **signs**, which keeps only the signs of the displacement components (directional information) while discarding magnitudes; (3) **value_only**, which collapses Z to the scalar V^* , making it perfectly value-sufficient yet highly action-insufficient; and (4) **distances**, which encodes per-coordinate goal distances, remaining value-sufficient while discarding the directional information required to select actions.

Δ_A and Δ_V are not structurally coupled. Figure 3(a) places each representation in the (Δ_V, Δ_A) plane and col-

ors points by the success rate under π_ϕ . Before turning to performance, the result illustrates that the two information losses Δ_A and Δ_V capture different aspects and need not move together. Importantly, we are *not* asserting that Δ_A and Δ_V are uncorrelated as random variables: when the representation ϕ is treated as random, $\Delta_A(\phi)$ and $\Delta_V(\phi)$ are induced random variables, and their distributions highly depend on the prior over ϕ (here, the representation library and sampling procedure). Since any finite library cannot cover the distribution over all possible representation functions, our goal is not to characterize these distributions in general. Rather, our claim is *structural*: driving Δ_V down does not, in general, force Δ_A down. A representation may preserve action-relevant structure while discarding value-relevant details (small Δ_A but large Δ_V), or preserve value-determining signals while collapsing action-distinguishing information (small Δ_V but large Δ_A). This experiment makes this decoupling explicit by exhibiting representations that realize each regime.

Success aligns with the action-sufficiency gap. Across the representation library, success correlates much more strongly with Δ_A than with Δ_V : representations that retain action-relevant goal information (small Δ_A) tend to succeed even when they discard value-relevant details, as illustrated by **signs**. Conversely, value-preserving representations can still fail when they collapse action distinctions: **value_only** retains V^* but cannot disambiguate goals that share the same value, while **distances** improves by preserving goal distances yet remains limited without directional cues. In contrast, **full** succeeds by preserving both.

For value-sufficient ϕ , $I(A; Z | S, V)$ captures the remaining failure mode. Figure 3(b) focuses on representations that are (near-) value-sufficient ($\Delta_V < 0.2$) and plots success rates against $I(A; Z | S, V)$, which measures how much Z disambiguates optimal actions within (S, V) level sets. Within this approximately value-sufficient regime, the remaining performance differences are explained by within-level-set action ambiguity, consistent with the trends observed for the baselines discussed above.

Overall, Discrete Cube provides an exact demonstration that value preservation alone does not ensure controllability: success under the mixed policy π_ϕ tracks the action gap Δ_A , and among (near-) value-sufficient representations it is further governed by the within-level-set disambiguation term $I(A; Z | S, V)$.

7. Method: Actor-Based Goal Representations and Approximate Action Sufficiency

The preceding sections demonstrate that value-shaped representations can fail for low-level control by discarding action-relevant information within value level sets. This mo-

tivates learning a goal representation that is directly aligned with action prediction.

7.1. Training vs. Deployment in Hierarchical Control

A key subtlety in hierarchical policy architecture is that the context available to the low-level policy differs between training and deployment. In a deployed hierarchical policy, the low-level policy is not assumed to have direct access to the ground-truth (sub)goal it must pursue. This is because, in many tasks, the specific intermediate subgoal (or its optimal representation) is not provided externally; instead, the low-level policy acts only on the current state and the subgoal representation predicted by the high-level policy.

During training, however, the availability of the full trajectory allows us to derive the target subgoal G_{sub} . Consequently, the low-level policy can condition on G_{sub} (or effectively G , as subgoals reside in the same space as final goals) during the learning phase. This discrepancy is crucial: *It allows us to learn a goal encoder from the full goal G during training and use the same representation space to condition the low-level policy on subgoals at deployment.*

7.2. Actor-Based Goal Representations

We capture the training-time access to G by structuring the full architecture of the low-level policy as:

$$\pi_\theta(\cdot | S, Z), \quad Z = \phi(S, G), \quad (8)$$

where ϕ is a goal encoder learned jointly with the policy head parameters θ . We train (θ, ϕ) jointly by minimizing the negative log-likelihood (NLL) loss³:

$$\mathcal{L}_{\text{act}}(\theta, \phi) := \mathbb{E}[-\log \pi_\theta(A | S, \phi(S, G))]. \quad (9)$$

Importantly, the low-level policy accesses the full goal G **only during training** to learn (θ, ϕ) . At deployment, we detach the encoder ϕ , and the policy π_θ conditions directly on a subgoal representation Z_{sub} predicted by the high-level policy, rather than on the true final goal.

As discussed in Section 3, we refer to the encoder learned via this policy optimization objective as an *actor-based goal representation* ϕ_A . In contrast, standard Hierarchical methods for GCRL (Park et al., 2023; 2025d) typically learn *value-based representations* ϕ_V via value estimation objectives (e.g., temporal difference learning).

7.3. Near-Optimal NLL Implies Approximate Action Sufficiency

We now show that learning a low-level policy formulated in this way through minimizing actor NLL naturally induces action-sufficient ϕ . Detailed proofs are provided in

³For exposition, we assume expert data sampled from the optimal goal-conditioned action law $P(A | S, G)$. While direct access to such an oracle unavailable, this is approximately realized in practice by advantage-weighted regression (AWR) objectives that concentrate probability mass on near-optimal actions.

Appendix H.

In Section 4, we defined the conditional KL risk (Eq. (5)) as the fundamental quantity to minimize for optimal control. The following lemma connects this theoretical risk to our tractable training objective.

Lemma 7.1 (Decomposition of Actor NLL). *For any (θ, ϕ) with $Z = \phi(S, G)$, the actor NLL $\mathcal{L}_{\text{act}}(\theta, \phi)$ decomposes as:*

$$\mathcal{L}_{\text{act}}(\theta, \phi) = H(A | S, G) + \mathcal{R}(\pi_\theta; \phi), \quad (10)$$

where $\mathcal{R}(\pi_\theta; \phi)$ is the conditional KL risk defined in Eq. (5).

Crucially, the entropy term $H(A | S, G)$ is fixed by the environment and data distribution; it is irreducible with respect to optimization. Therefore, minimizing the actor NLL $\mathcal{L}_{\text{act}}(\theta, \phi)$ is equivalent to minimizing the conditional KL risk $\mathcal{R}(\pi_\theta; \phi)$. By combining Lemma 7.1 with the risk decomposition in Proposition 4.1, we obtain our main theoretical result: *achieving near-optimal NLL guarantees that the learned representation is approximately action-sufficient*.

Theorem 7.2 (Near-Optimal Actor NLL Implies Approximate Action Sufficiency). *For any (θ, ϕ) with $Z = \phi(S, G)$, the action sufficiency gap $\Delta_A = I(A; G | S, Z)$ is bounded by the excess risk:*

$$\Delta_A \leq \mathcal{L}_{\text{act}}(\theta, \phi) - H(A | S, G). \quad (11)$$

In particular, if the actor NLL is near-optimal such that $\mathcal{L}_{\text{act}}(\theta, \phi) \leq H(A | S, G) + \varepsilon$, then

$$\Delta_A \leq \varepsilon, \quad (12)$$

i.e., Z is ε -approximately action-sufficient.

7.4. Theoretical Interpretation and Practical Implications

Theorem 7.2 implies that standard NLL minimization serves a dual purpose: it optimizes the low-level policy while simultaneously forcing the representation ϕ to retain all goal information necessary for action prediction. In particular, assuming the parameterized policy class in Eq. (8) has sufficient expressivity to approximate the optimal kernel $P(A | S, G)$, minimizing actor NLL drives the excess risk to zero, thereby ensuring $\Delta_A \rightarrow 0$.

While grounded in rigorous analysis, the proposed method is **remarkably simple in practice**: we attach a goal encoder $\phi(S, G)$ directly to the input of the low-level policy and jointly minimize the actor NLL.

Our analysis suggests that actor-based representations offer a principled alternative when the primary goal is accurate control. By retaining the structural information necessary

Table 1. Success rate comparison of offline GCRL algorithms across cube tasks. Environments are subdivided by noise conditions (play vs. noisy). Results are averaged across 8 seeds.

Method	Goal Rep.	cube-double		cube-triple		cube-quadruple	
		play	noisy	play	noisy	play	noisy
HIQL ^{OTA}	Value Rep. (ϕ_V)	0.26	0.25	0.16	0.09	0.01	0.02
HIQL ^{OTA}	Actor Rep. (ϕ_A)	0.42	0.29	0.41	0.19	0.28	0.08
H-Flow ^{OTA}	Value Rep. (ϕ_V)	0.26	0.28	0.15	0.10	0.01	0.01
H-Flow ^{OTA}	Actor Rep. (ϕ_A)	0.43	0.33	0.45	0.23	0.25	0.11
GCIQL	–	0.69	0.13	0.30	0.14	0.01	0.00
GCIVL	–	0.36	0.20	0.08	0.14	0.00	0.00

Table 2. Comparison of success rates between the learned representations and original goals $g \in \mathcal{G}$ (without encoder).

Goal Rep.	cube-double		cube-triple	
	play	noisy	play	noisy
No Rep.	0.27	0.24	0.23	0.06
Value Rep. (ϕ_V)	0.26	0.25	0.16	0.10
Actor Rep. (ϕ_A)	0.42	0.29	0.41	0.19

for action prediction, this approach avoids the potential information loss of value-based representations.

8. Experiment

We investigate the impact of various representations by integrating them into HIQL (Park et al., 2023), a versatile hierarchical framework for GCRL, using **OGBench** (Park et al., 2025a) as our testbed—a challenging benchmark for offline GCRL with high-dimensional observations. Specifically, we focus on cube tasks, which require the agent to precisely rearrange multiple objects into target configurations, thereby serving as a rigorous test for control capabilities. To assess the robustness of representations against sub-optimal demonstrations, we utilize both the `play` (clean) and `noisy` datasets. Furthermore, we compare our approach against standard offline GCRL baselines GCIQL and GCIVL (Kostrikov et al., 2022). All results are reported as success rates averaged over 8 random seeds.

Performance on Manipulation Tasks. Table 1 demonstrates that substituting the value-based representation (ϕ_V) with our actor-based representation (ϕ_A) yields consistent performance gains, particularly in high-difficulty tasks (e.g., cube-quadruple) where baselines collapse. Furthermore, to address the limited expressivity of unimodal Gaussian policies used in standard HIQL, we employ flow matching (Kang et al., 2023; Park et al., 2025c) as a generative backbone (Hierarchical Flow, H-Flow^{OTA}). Consequently, the combination of H-Flow^{OTA} and ϕ_A leads to improved results by handling the multimodal action distributions required for these tasks.

Necessity of Goal Representation. Theoretically, utilizing the original goal $g \in \mathcal{G}$ ensures maximum action sufficiency. However, Table 2 reveals that it is not empirically optimal. As noted by Park et al. (2023), high-dimensional goals often contain nuisance information that makes direct subgoal prediction inefficient. While value-based representations compress this noise, they ultimately degrade performance by discarding control-relevant features. In contrast, our actor-based representation resolves this trade-off by filtering out nuisance information while strictly preserving the structure necessary for control.

9. Conclusion

We formally defined **action sufficiency**, identifying it as a critical requirement for goal representations for hierarchical control in offline GCRL. We demonstrated that widely used value-based representations often discard essential action information, whereas our proposed **actor-based goal representations** are provably approximately action-sufficient. Empirical results on both the discrete domain and complex manipulation tasks confirm that satisfying this property significantly enhances hierarchical control performance.

9.1. Limitations and Future Directions

Gap between theory and practice. Our theoretical analysis assumes access to the true distribution, whereas offline learning relies on static datasets. Consequently, limited data coverage may widen the gap between theoretical guarantees and practical action sufficiency.

Sufficiency vs. Predictability. While action sufficiency is necessary for the low-level policy, it is not sufficient for the entire hierarchy. As the goal representation acts as an interface between planning and control, it must also be compact and predictable for the high-level policy (as indicated in Table 2). Future work should explore balancing action-relevant information with the compressibility required for efficient high-level planning.

References

Ahn, H., Choi, H., Han, J., and Moon, T. Option-aware temporally abstracted value for offline goal-conditioned reinforcement learning. In *The Thirty-ninth Annual Conference on Neural Information Processing Systems*, 2025.

Andrychowicz, M., Wolski, F., Ray, A., Schneider, J., Fong, R., Welinder, P., McGrew, B., Tobin, J., Pieter Abbeel, O., and Zaremba, W. Hindsight experience replay. In *Advances in Neural Information Processing Systems (NeurIPS)*, 2017.

Chane-Sane, E., Schmid, C., and Laptev, I. Goal-conditioned reinforcement learning with imagined subgoals. In *International Conference on Machine Learning (ICML)*, 2021.

Chebotar, Y., Hausman, K., Lu, Y., Xiao, T., Kalashnikov, D., Varley, J., Irpan, A., Eysenbach, B., Julian, R., Finn, C., et al. Actionable models: Unsupervised offline reinforcement learning of robotic skills. In *International Conference on Machine Learning (ICML)*, 2021.

Dayan, P. and Hinton, G. E. Feudal reinforcement learning. In *Advances in Neural Information Processing Systems (NeurIPS)*, 1992.

Ding, Y., Florensa, C., Abbeel, P., and Philipp, M. Goal-conditioned imitation learning. In *Advances in Neural Information Processing Systems (NeurIPS)*, 2019.

Durugkar, I., Tec, M., Niekum, S., and Stone, P. Adversarial intrinsic motivation for reinforcement learning. In *Advances in Neural Information Processing Systems (NeurIPS)*, 2021.

Eysenbach, B., Salakhutdinov, R. R., and Levine, S. Search on the replay buffer: Bridging planning and reinforcement learning. In *Advances in Neural Information Processing Systems (NeurIPS)*, 2019.

Eysenbach, B., Zhang, T., Levine, S., and Salakhutdinov, R. R. Contrastive learning as goal-conditioned reinforcement learning. In *Advances in Neural Information Processing Systems (NeurIPS)*, 2022.

Gong, X., Dawei, F., Xu, K., Ding, B., and Wang, H. Goal-conditioned on-policy reinforcement learning. In *Advances in Neural Information Processing Systems (NeurIPS)*, 2024.

Gürtler, N., Büchler, D., and Martius, G. Hierarchical reinforcement learning with timed subgoals. In *Advances in Neural Information Processing Systems (NeurIPS)*, 2021.

Hong, Z.-W., Yang, G., and Agrawal, P. Bilinear value networks, 2023. URL <https://arxiv.org/abs/2204.13695>.

Huang, Z., Liu, F., and Su, H. Mapping state space using landmarks for universal goal reaching. In *Advances in Neural Information Processing Systems (NeurIPS)*, 2019.

Jiang, Y., Gu, S. S., Murphy, K. P., and Finn, C. Language as an abstraction for hierarchical deep reinforcement learning. In *Advances in Neural Information Processing Systems (NeurIPS)*, 2019.

Jurgenson, T., Avner, O., Groshev, E., and Tamar, A. Subgoal trees a framework for goal-based reinforcement learning. In *International conference on machine learning (ICML)*, 2020.

Kang, B., Ma, X., Du, C., Pang, T., and Yan, S. Efficient diffusion policies for offline reinforcement learning. In *International Conference on Learning Representations (ICLR)*, 2023.

Kim, J., Seo, Y., and Shin, J. Landmark-guided subgoal generation in hierarchical reinforcement learning. In *Advances in Neural Information Processing Systems (NeurIPS)*, 2021.

Kim, J., Seo, Y., Ahn, S., Son, K., and Shin, J. Imitating graph-based planning with goal-conditioned policies. In *International Conference on Learning Representations (ICLR)*, 2023.

Kostrikov, I., Nair, A., and Levine, S. Offline reinforcement learning with implicit q-learning. In *International Conference on Learning Representations (ICLR)*, 2022.

Kulkarni, T. D., Narasimhan, K., Saeedi, A., and Tenenbaum, J. Hierarchical deep reinforcement learning: Integrating temporal abstraction and intrinsic motivation. In *Advances in Neural Information Processing Systems (NeurIPS)*, 2016.

Liu, G., Tang, M., and Eysenbach, B. A single goal is all you need: Skills and exploration emerge from contrastive rl without rewards, demonstrations, or subgoals. In *International Conference on Learning Representations (ICLR)*, 2025.

Liu, M., Zhu, M., and Zhang, W. Goal-conditioned reinforcement learning: Problems and solutions. In *International Joint Conference on Artificial Intelligence (IJCAI)*, 2022.

Ma, J. Y., Yan, J., Jayaraman, D., and Bastani, O. Offline goal-conditioned reinforcement learning via f -advantage regression. In *Advances in Neural Information Processing Systems (NeurIPS)*, 2022.

Ma, Y. J., Sodhani, S., Jayaraman, D., Bastani, O., Kumar, V., and Zhang, A. Vip: Towards universal visual reward and representation via value-implicit pre-training. In

International Conference on Learning Representations (ICLR), 2023.

Myers, V., Ji, C., and Eysenbach, B. Horizon generalization in reinforcement learning. In *International Conference on Learning Representations (ICLR)*, 2025.

Nachum, O., Gu, S. S., Lee, H., and Levine, S. Data-efficient hierarchical reinforcement learning. In *Advances in Neural Information Processing Systems (NeurIPS)*, 2018.

Nair, A., Gupta, A., Dalal, M., and Levine, S. Awac: Accelerating online reinforcement learning with offline datasets. *arXiv preprint arXiv:2006.09359*, 2020.

Nair, S. and Finn, C. Hierarchical foresight: Self-supervised learning of long-horizon tasks via visual subgoal generation. In *International Conference on Learning Representations (ICLR)*, 2020.

Nasiriany, S., Pong, V., Lin, S., and Levine, S. Planning with goal-conditioned policies. In *Advances in Neural Information Processing Systems (NeurIPS)*, 2019.

Park, S., Ghosh, D., Eysenbach, B., and Levine, S. Hiql: Offline goal-conditioned rl with latent states as actions. In *Advances in Neural Information Processing Systems (NeurIPS)*, 2023.

Park, S., Kreiman, T., and Levine, S. Foundation policies with hilbert representations. In *International Conference on Machine Learning (ICML)*, 2024.

Park, S., Frans, K., Eysenbach, B., and Levine, S. Ogbench: Benchmarking offline goal-conditioned rl. In *International Conference on Learning Representations (ICLR)*, 2025a.

Park, S., Frans, K., Mann, D., Eysenbach, B., Kumar, A., and Levine, S. Horizon reduction makes RL scalable. In *The Thirty-ninth Annual Conference on Neural Information Processing Systems*, 2025b.

Park, S., Li, Q., and Levine, S. Foundation policies with hilbert representations. In *International Conference on Machine Learning (ICML)*, 2025c.

Park, S., Mann, D., and Levine, S. Dual goal representations, 2025d. URL <https://arxiv.org/abs/2510.06714>.

Pateria, S., Subagdja, B., Tan, A.-h., and Quek, C. Hierarchical reinforcement learning: A comprehensive survey. *ACM Computing Surveys (CSUR)*, 54(5):1–35, 2021.

Peng, X. B., Kumar, A., Zhang, G., and Levine, S. Advantage-weighted regression: Simple and scalable off-policy reinforcement learning. *arXiv preprint arXiv:1910.00177*, 2019.

Precup, D. *Temporal abstraction in reinforcement learning*. University of Massachusetts Amherst, 2000.

Ren, Z., Dong, K., Zhou, Y., Liu, Q., and Peng, J. Exploration via hindsight goal generation. In *Advances in Neural Information Processing Systems (NeurIPS)*, 2019.

Schaul, T., Horgan, D., Gregor, K., and Silver, D. Universal value function approximators. In *International Conference on Machine Learning (ICML)*, 2015.

Sermanet, P., Lynch, C., Chebotar, Y., Hsu, J., Jang, E., Schaal, S., and Levine, S. Time-contrastive networks: Self-supervised learning from video, 2018. URL <https://arxiv.org/abs/1704.06888>.

Sikchi, H., Chitnis, R., Touati, A., Geramifard, A., Zhang, A., and Niekum, S. Score models for offline goal-conditioned reinforcement learning. In *International Conference on Learning Representations (ICLR)*, 2024.

Vezehnevets, A. S., Osindero, S., Schaul, T., Heess, N., Jaderberg, M., Silver, D., and Kavukcuoglu, K. Feudal networks for hierarchical reinforcement learning. In *International conference on machine learning (ICML)*, 2017.

Wang, Q., Xiong, J., Han, L., Liu, H., Zhang, T., et al. Exponentially weighted imitation learning for batched historical data. In *Advances in Neural Information Processing Systems (NeurIPS)*, 2018.

Wang, T., Torralba, A., Isola, P., and Zhang, A. Optimal goal-reaching reinforcement learning via quasimetric learning. In *International Conference on Machine Learning (ICML)*, 2023.

Wu, C., Hu, H., Yang, Y., Zhang, N., and Zhang, C. Planning, fast and slow: online reinforcement learning with action-free offline data via multiscale planners. In *International Conference on Machine Learning (ICML)*, 2024.

Yang, R., Lu, Y., Li, W., Sun, H., Fang, M., Du, Y., Li, X., Han, L., and Zhang, C. Rethinking goal-conditioned supervised learning and its connection to offline rl. In *International Conference on Learning Representations (ICLR)*, 2022.

Zhang, L., Yang, G., and Stadie, B. C. World model as a graph: Learning latent landmarks for planning. In *International Conference on Machine Learning (ICML)*, 2021.

Zhang, T., Guo, S., Tan, T., Hu, X., and Chen, F. Generating adjacency-constrained subgoals in hierarchical reinforcement learning. In *Advances in Neural Information Processing Systems (NeurIPS)*, 2020.

Zheng, S., Bai, C., Yang, Z., and Wang, Z. How does goal relabeling improve sample efficiency? In *International Conference on Machine Learning (ICML)*, 2024.

Appendix

A. Preliminary

Hierarchical Implicit Q-Learning (HIQL) & Temporal Abstraction. A central challenge in GCRL is accurately estimating value functions for distant goals, which is crucial for solving long-horizon and temporally extended tasks (Huang et al., 2019; Kim et al., 2021; Park et al., 2023). To mitigate this difficulty, HIQL (Park et al., 2023) introduces a hierarchical policy framework built upon a value function learned via Implicit Q-Learning (IQL) (Kostrikov et al., 2022). This hierarchical structure allows the agent to select meaningful actions even when value estimates for faraway goals are inaccurate or noisy. However, as deeply studied in (Park et al., 2025b; Ahn et al., 2025), the value learning scheme in IQL failed to capture the long-horizon reward signal effectively. To solve this problem, (Park et al., 2025b; Ahn et al., 2025) adopt temporal abstraction scheme which updates the value over n step target to decrease the effective horizon from start state S to goal g .

Specifically, HIQL with temporal abstraction learns a goal-conditioned state-value function V by minimizing the following expectile regression objective:

$$\mathcal{L}(V) = \mathbb{E}_{(s, s_n) \sim \mathcal{D}, g \sim p(g)} [L_2^\tau(r(s_n, g) + \gamma \bar{V}(s_n, g) - V(s, g))], \quad (13)$$

where the expectile loss is defined as $L_2^\tau(u) = |\tau - \mathbf{1}(u < 0)|u^2$ with $\tau > 0.5$, and \bar{V} denotes a target value network.⁴

Unlike prior studies (Andrychowicz et al., 2017; Chane-Sane et al., 2021; Wang et al., 2023; Park et al., 2023; Wu et al., 2024), we instead adopt an option-aware sparse goal-reaching reward (Ahn et al., 2025; Park et al., 2025b) of the form $r(s_n, g) = -\mathbf{1}\{s_n \neq g\}$, where s_n denotes n step forward state from the state s . Under this reward structure, the magnitude of the optimal value function $|V^*(s, g)|$ corresponds to the *discounted temporal distance with temporal abstraction*, representing discounted estimate of the minimum number of environment steps required to reach goal g from state s with temporal abstraction.

HIQL decouples policy extraction into two hierarchical components. The high-level policy $\pi^h(s_{t+k} | s_t, g)$ proposes a k -step subgoal that guides progress toward the target goal, while the low-level policy $\pi^\ell(a_t | s_t, s_{t+k})$ generates primitive actions to reach the proposed subgoal. Both policies are learned using advantage-weighted regression (AWR) (Wang et al., 2018; Peng et al., 2019; Nair et al., 2020), with objectives given by

$$\mathcal{J}(\pi^h) = \mathbb{E}_{(s_t, s_{t+k}, g) \sim \mathcal{D}} [\alpha^h \cdot \log \pi^h(s_{t+k} | s_t, g)], \quad (14)$$

$$\mathcal{J}(\pi^\ell) = \mathbb{E}_{(s_t, a_t, s_{t+1}, s_{t+k}) \sim \mathcal{D}} [\alpha^\ell \cdot \log \pi^\ell(a_t | s_t, s_{t+k})], \quad (15)$$

where $\alpha^h = \exp(\beta^h A^h(s_t, s_{t+k}, g))$, $\alpha^\ell = \exp(\beta^\ell A^\ell(s_t, s_{t+1}, s_{t+k}))$, β^h and β^ℓ are inverse temperature parameters. The high-level advantage is defined as $A^h(s_t, s_{t+k}, g) = V^h(s_{t+k}, g) - V^h(s_t, g)$, and the low-level advantage as $A^\ell(s_t, s_{t+1}, s_{t+k}) = V^\ell(s_{t+1}, s_{t+k}) - V^\ell(s_t, s_{t+k})$. Note that, since the high level policy π^h should plan the subgoal properly when the distance between s and g is quite large, and the low level policy π^ℓ only works on short-horizon scenario, we adopt large n for V^h and $n = 1$ for V^ℓ .

In practice, HIQL learns goal representation $\phi([s, g])$ when training the value function V^h and V^ℓ . By leveraging the learned representation $\phi([s, g])$, both π^h and π^ℓ use $\phi([s, s_{t+k}])$ as proxy of subgoal s_{t+k} .

In this paper, we deeply analyze the role of using $\phi([s, s_{t+k}])$ when learning both policy π^h and π^ℓ , and we conclude that there can be failure mode for learning the policies when we use $\phi([s, s_{t+k}])$ learned from training the value function.

B. Related Work

Goal-Conditioned Reinforcement Learning (GCRL). Goal-conditioned reinforcement learning (GCRL) studies the problem of learning policies that can reach *arbitrary* goal states from given initial states, rather than optimizing performance for a single predefined task (Schaul et al., 2015; Liu et al., 2022). In this work, we focus on the offline GCRL setting (Chebotar et al., 2021; Ma et al., 2022; Park et al., 2023; Sikchi et al., 2024; Park et al., 2025a;b), where goal-conditioned policies are learned exclusively from fixed, pre-collected datasets without additional interaction with the environment.

A key challenge in offline GCRL arises from the sparse and delayed rewards inherent to goal-reaching tasks. To alleviate this issue, prior works have extensively employed hindsight data relabeling techniques (Andrychowicz et al., 2017; Ren

⁴Due to the overestimation issues inherent in IQL, we assume deterministic environment dynamics in this work.

et al., 2019; Zheng et al., 2024). More recently, imitation learning and value-based approaches have been investigated as principled ways to exploit suboptimal or heterogeneous datasets (Ding et al., 2019; Yang et al., 2022; Gong et al., 2024). In these methods, value functions are commonly learned via temporal-difference (TD) learning (Kostrikov et al., 2022; Park et al., 2024), or through alternative formulations such as state-occupancy matching (Ma et al., 2022; Durugkar et al., 2021), contrastive representation learning (Ma et al., 2023; Eysenbach et al., 2022; Liu et al., 2025), and quasimetric-based distance learning (Wang et al., 2023; Myers et al., 2025).

Hierarchical Reinforcement Learning. Learning to achieve long-horizon goals has long been recognized as a central challenge in reinforcement learning and, more recently, in GCRL (Precup, 2000; Patera et al., 2021; Kim et al., 2021; Park et al., 2023). Hierarchical reinforcement learning (HRL) addresses this challenge by decomposing decision-making across multiple temporal or abstraction levels. Existing HRL approaches can be broadly categorized into two paradigms. The first category performs graph-based planning over the state space or learned abstractions (Eysenbach et al., 2019; Huang et al., 2019; Zhang et al., 2020; Kim et al., 2021; Zhang et al., 2021; Kim et al., 2023), while the second relies on waypoint- or subgoal-based decomposition, where high-level policies generate intermediate targets that guide low-level policies (Dayan & Hinton, 1992; Kulkarni et al., 2016; Vezhnevets et al., 2017; Nachum et al., 2018; Jiang et al., 2019; Görtler et al., 2021; Nasiriany et al., 2019; Nair & Finn, 2020; Jurgenson et al., 2020; Chane-Sane et al., 2021; Park et al., 2023; Wu et al., 2024).

While graph-based planning methods provide explicit long-term reasoning capabilities, they often incur substantial computational overhead and architectural complexity. Waypoint-based approaches offer a more scalable alternative, but their performance critically depends on the accuracy of value estimates used to propose subgoals. In long-horizon settings, value estimation errors can accumulate when the agent is far from the target goal, leading to ineffective or misleading subgoal generation.

Learning Goal Representations Several approaches integrate goal representation learning into value optimization; for instance, (Sermanet et al., 2018) uses time-step proximity for metric learning, while (Eysenbach et al., 2022) employs contrastive learning across trajectories. Building on the empirical success of (Hong et al., 2023), (Park et al., 2023) learns representations by concatenating states and goals but lacks a systematic analysis of this mechanism. To address this, (Park et al., 2025d) proposed a framework to measure temporal distance, interpreting it through value function optimization. In contrast, we argue that while policy learning requires action-sufficient features, value learning is inherently limited in extracting them. This directly contradicts the claims in (Park et al., 2025d), a point we analyze further from an information-theoretic perspective.

C. Additional Discussions

C.1. Justification for State-Dependent Representation

In Section 4, we defined the goal representation as a function of both the current state and the goal, denoted by $Z = \phi(S, G)$. While goal-conditioned reinforcement learning often utilizes goal-only encoders (*i.e.*, $Z = \psi(G)$; see, *e.g.*, Park et al., 2025d), we argue that the state-dependent formulation is a more general and architecturally natural choice for hierarchical control.

We provide a detailed justification for this design choice based on three perspectives: mathematical subsumption, theoretical invariance, and architectural consistency.

C.1.1. MATHEMATICAL SUBSUMPTION

First and foremost, the set of state-dependent encoders strictly subsumes the set of goal-only encoders. A representation that depends solely on the goal is simply a special case of our formulation where the dependence on S is trivial.

Formally, let Ψ be the set of measurable functions mapping $\mathcal{G} \rightarrow \mathcal{Z}$. For any goal-only encoder $\psi \in \Psi$, we can construct an equivalent state-dependent encoder ϕ as follows:

$$\phi(S, G) := (\psi \circ \Pi_{\mathcal{G}})(S, G),$$

where $\Pi_{\mathcal{G}} : \mathcal{S} \times \mathcal{G} \rightarrow \mathcal{G}$ is the standard canonical projection defined by $\Pi_{\mathcal{G}}(s, g) = g$.

This implies that our analysis of $\phi(S, G)$ entails no loss of generality; any result derived for the state-dependent case naturally applies to goal-only encoders by restricting the function class. By allowing ϕ to access S , we simply expand the hypothesis space for the representation, potentially allowing for more compact encodings (*e.g.*, relative goal coordinates)

that are impossible with $\psi(G)$ alone.

C.1.2. INVARIANCE OF ACTION SUFFICIENCY

One might ask whether introducing S into ϕ complicates the definition of action sufficiency. We emphasize that our core definition is agnostic to the internal structure of ϕ .

Recall the definition of action sufficiency:

$$I(A; G | S, Z) = 0.$$

This condition requires that Z , *in conjunction with* S , allows for the optimal prediction of A . Even if Z were derived solely from G (*i.e.*, $Z = \psi(G)$), the conditioning on S in the mutual information term remains present. Therefore, the theoretical validity of our decomposition and the resulting sufficiency condition holds regardless of whether the encoder explicitly takes S as input.

C.1.3. ARCHITECTURAL CONSISTENCY IN HIERARCHICAL METHODS

Finally, from a practical standpoint, the state-dependent formulation aligns naturally with the information structure of Hierarchical methods for GCRL. In this framework, all major components inherently possess access to the current state S :

- The **High-Level Policy** $\pi^h(G_{\text{sub}} | S, G)$ observes S to decide which subgoal is reachable.
- The **Low-Level Policy** $\pi^\ell(A | S, Z)$ observes S to execute immediate actions.
- The **Value Function** $V(S, G)$ (or $V(S, Z)$) observes S to estimate expected returns.

Since the policy side already conditions on S , “contextualizing” the encoder side with S creates a symmetric information structure. For instance, in navigation tasks, encoding a goal as a “relative vector from the current state” (which requires access to both S and G) is often far more efficient and robust than encoding absolute coordinates. Our formulation $\phi(S, G)$ formally accommodates such relative representations, whereas a rigid $\psi(G)$ formulation would exclude them.

C.2. Limitations of Goal-Only Value-Based Representations

Prior work, *e.g.*, Park et al. (2023; 2025d), studies goal representations of the form $Z = \psi(G)$ constructed from value information, arguing that such value-based representations can be sufficient for predicting goal-conditioned behavior. Here, we analyze the limitations of this approach, specifically showing that under reasonable assumptions, strict value sufficiency for goal-only representations forces the retention of *all* goal information, including nuisance factors.

C.2.1. ASSUMPTIONS AND DEFINITIONS

We assume the value target $V(s, g)$ uniquely identifies the goal when the agent is at the goal state.

Assumption C.1 (Zero if and only if identity). For all $s, g \in \mathcal{S} = \mathcal{G}$,

$$V(s, g) = 0 \iff s = g.$$

Previous works effectively utilize a condition slightly stronger than our information-theoretic value sufficiency, which we formalize as *strict value sufficiency*.

Definition C.2 (Strict value sufficiency). A goal representation $Z = \psi(G)$ is *strictly value-sufficient* if there exists a measurable function \tilde{v} such that

$$V(s, g) = \tilde{v}(s, \psi(g)) \quad \text{for all } (s, g) \in \mathcal{S} \times \mathcal{G}.$$

C.2.2. INJECTIVITY AND INFORMATION EQUIVALENCE

Under Assumption C.1, strict value sufficiency implies that ψ must be injective. This result formalizes the intuition that if two distinct goals map to the same representation, their value functions must be identical everywhere, leading to a contradiction at the goal states.

C.2.3. INJECTIVITY AND INFORMATION EQUIVALENCE

We first establish a general measure-theoretic lemma stating that an injective representation allows for the perfect reconstruction of the original variable, thereby generating the same σ -algebra.

Lemma C.3 (Injectivity implies information equivalence). *Let $Z = \psi(G)$ where $\psi : \mathcal{G} \rightarrow \mathcal{Z}$ is a measurable function between standard Borel spaces. If ψ is injective, then*

$$\sigma(G) = \sigma(Z) \quad (\text{modulo null sets}),$$

where $\sigma(X)$ denotes the σ -algebra generated by the random variable X .

Proof. Since Z is a function of G , the inclusion $\sigma(Z) \subseteq \sigma(G)$ holds trivially. Conversely, for standard Borel spaces, an injective measurable function maps measurable sets to measurable sets and possesses a measurable inverse on its range. Thus, G can be recovered from Z almost surely via the inverse map ψ^{-1} , implying $\sigma(G) \subseteq \sigma(Z)$. Therefore, the two σ -algebras coincide. \square

Using this lemma, we now show that under strict value sufficiency, the representation must preserve all goal information. The proof proceeds by first showing that strict value sufficiency forces ψ to be injective.

Proposition C.4 (Strict value sufficiency implies $\sigma(G) = \sigma(Z)$). *Assume $Z = \psi(G)$ is strictly value-sufficient. Then*

$$\sigma(G) = \sigma(Z) \quad (\text{modulo null sets}).$$

Proof. First, we show that ψ is injective on \mathcal{G} . Suppose for the sake of contradiction that there exist distinct goals $g_1 \neq g_2$ such that $\psi(g_1) = \psi(g_2)$. By strict value sufficiency (Definition C.2), the value function must satisfy:

$$V(s, g_1) = \tilde{v}(s, \psi(g_1)) = \tilde{v}(s, \psi(g_2)) = V(s, g_2)$$

for all states $s \in \mathcal{S}$. Evaluating this at $s = g_1$, we have $V(g_1, g_1) = V(g_1, g_2)$. By Assumption C.1, $V(g_1, g_1) = 0$, which implies $V(g_1, g_2) = 0$. Applying Assumption C.1 again to the right-hand side necessitates $g_1 = g_2$, which contradicts our assumption that $g_1 \neq g_2$.

Thus, ψ must be injective. Applying Lemma C.3, we conclude that $\sigma(G) = \sigma(Z)$. \square

C.2.4. DISCUSSION

Proposition C.4 demonstrates that under strict value sufficiency, a goal-only representation $Z = \psi(G)$ must retain *exactly* the same information as the original goal G . This is often undesirable because high-dimensional goals typically contain nuisance information that is irrelevant for control. Forcing the representation to preserve all goal information contradicts the principle of abstraction in hierarchical learning, where the goal representation should ideally act as a compressed interface passing only relevant information to the low-level controller.

Unlike this rigid requirement, our proposed framework isolates *action-relevant* information via action sufficiency, allowing for many-to-one mappings that discard nuisance factors while preserving the control-relevant content necessary for optimal policy execution.

D. Proofs for Section 4

In this section, we provide the formal derivations for the Conditional KL Risk Decomposition (Proposition 4.1) and discuss the theoretical implications of action sufficiency.

D.1. Goal-Marginalization Lemma

Before proving the main decomposition, we establish a useful lemma characterizing the relationship between the optimal policy conditioned on the raw goal G and the optimal policy conditioned on the representation Z . This justifies viewing $P(\cdot | S, Z)$ as the posterior mixture of the expert policy.

Lemma D.1 (Goal-Marginalization). *Let $Z = \phi(S, G)$ be a deterministic representation. The conditional distribution of the optimal action A given (S, Z) satisfies the following marginalization property:*

$$P(A \in B | S, Z) = \mathbb{E} [P(A \in B | S, G) | S, Z] \tag{16}$$

for any measurable set $B \subseteq \mathcal{A}$.

Proof. By the tower property of conditional expectation and noting that Z is $\sigma(S, G)$ -measurable (since $Z = \phi(S, G)$), we have:

$$\begin{aligned}\mathbb{E}[\mathbf{1}\{A \in B\} | S, Z] &= \mathbb{E}\left[\mathbb{E}[\mathbf{1}\{A \in B\} | S, G, Z] \mid S, Z\right] \\ &= \mathbb{E}\left[\mathbb{E}[\mathbf{1}\{A \in B\} | S, G] \mid S, Z\right].\end{aligned}$$

The second equality holds because conditioning on (S, G) fully determines Z , making Z redundant in the inner expectation (i.e., $P(\cdot | S, G, Z) = P(\cdot | S, G)$). The left-hand side is $P(A \in B | S, Z)$ and the inner term on the right-hand side is $P(A \in B | S, G)$, which proves Eq. (16). \square

D.2. Proof of the Conditional KL Risk Decomposition

We now provide the proof for the decomposition of the conditional KL risk. We first recall the statement of the proposition:

Proposition D.2 (Conditional KL Risk Decomposition). *The risk $\mathcal{R}(\pi^\ell; \phi)$ decomposes into a modeling error term and a representation error term:*

$$\begin{aligned}\mathcal{R}(\pi^\ell; \phi) &= \underbrace{\mathbb{E}[D_{\text{KL}}(P(A|S, Z) \| \pi^\ell(A|S, Z))]}_{\text{Modeling Error}} \\ &\quad + \underbrace{I(A; G | S, Z)}_{\text{Representation Error}},\end{aligned}$$

where $I(\cdot; \cdot)$ denotes conditional mutual information.

Proof. Recall the definition of the risk from Eq. (5):

$$\mathcal{R}(\pi^\ell; \phi) = \mathbb{E}[D_{\text{KL}}(P(A|S, G) \| \pi^\ell(A|S, Z))].$$

We define the conditional mutual information term using its standard characterization. Since $Z = \phi(S, G)$ is deterministic, $P(A | S, G, Z) = P(A | S, G)$ almost surely, simplifying the mutual information to:

$$I(A; G | S, Z) = \mathbb{E}[D_{\text{KL}}(P(A | S, G) \| P(A | S, Z))]. \quad (17)$$

Now, consider the pointwise KL divergence inside the expectation of the risk \mathcal{R} . For fixed (s, g, z) , we decompose the log-likelihood ratio:

$$\begin{aligned}D_{\text{KL}}(P(\cdot | s, g) \| \pi^\ell(\cdot | s, z)) &= \int P(a | s, g) \log \frac{P(a | s, g)}{\pi^\ell(a | s, z)} da \\ &= \int P(a | s, g) \log \left(\frac{P(a | s, g)}{P(a | s, z)} \cdot \frac{P(a | s, z)}{\pi^\ell(a | s, z)} \right) da \\ &= \underbrace{\int P(a | s, g) \log \frac{P(a | s, g)}{P(a | s, z)} da}_{\text{(I)}} + \underbrace{\int P(a | s, g) \log \frac{P(a | s, z)}{\pi^\ell(a | s, z)} da}_{\text{(II)}}.\end{aligned}$$

We now take the expectation over (S, G) (and implicitly Z):

1. **Term (I):** The expectation of the first term corresponds exactly to Eq. (17), which is the **Representation Error** $I(A; G | S, Z)$.
2. **Term (II):** For the second term, we apply the law of iterated expectations, conditioning on (S, Z) :

$$\begin{aligned}\mathbb{E}_{S, G} \left[\int P(a | S, G) \log \frac{P(a | S, Z)}{\pi^\ell(a | S, Z)} da \right] \\ = \mathbb{E}_{S, Z} \left[\mathbb{E}_{G | S, Z} \left[\int P(a | S, G) \log \frac{P(a | S, Z)}{\pi^\ell(a | S, Z)} da \right] \right]\end{aligned}$$

$$\begin{aligned}
 &= \mathbb{E}_{S,Z} \left[\int \underbrace{\mathbb{E}_{G|S,Z}[P(a|S,G)]}_{P(a|S,Z) \text{ by Lemma D.1}} \log \frac{P(a|S,Z)}{\pi^\ell(a|S,Z)} da \right] \\
 &= \mathbb{E}_{S,Z} [D_{\text{KL}}(P(\cdot|S,Z) \parallel \pi^\ell(\cdot|S,Z))].
 \end{aligned}$$

This yields the **Modeling Error**.

Combining these two terms completes the proof. \square

D.3. Optimality of Action Sufficiency

The decomposition derived above allows us to formally state the conditions under which the control risk can be minimized to zero.

Corollary D.3 (Zero Minimal KL Risk \iff Action Sufficiency). *For a deterministic representation $Z = \phi(S, G)$, the following statements are equivalent:*

1. *The representation is action-sufficient: $I(A; G | S, Z) = 0$.*
2. *The minimum achievable risk is zero: $\inf_{\pi^\ell} \mathcal{R}(\pi^\ell; \phi) = 0$.*

Proof. From Proposition D.2, the risk is the sum of a non-negative modeling error and the representation error $\Delta_A = I(A; G | S, Z)$.

$$\inf_{\pi^\ell} \mathcal{R}(\pi^\ell; \phi) = \inf_{\pi^\ell} \left(\mathbb{E} [D_{\text{KL}}(P(A|S,Z) \parallel \pi^\ell(A|S,Z))] \right) + \Delta_A.$$

The modeling error is minimized to 0 if and only if $\pi^\ell(\cdot | S, Z) = P(\cdot | S, Z)$ almost surely. Thus, the infimum of the risk is exactly Δ_A . Consequently, the risk can be driven to zero if and only if $\Delta_A = 0$. \square

E. Proofs for Section 5

In this section, we provide the formal proofs characterizing the limitations of value-based representations, specifically showing how value sufficiency implies functional dependence yet fails to guarantee action sufficiency.

E.1. Equivalence of Value Sufficiency and Functional Dependence

We first establish that value sufficiency is equivalent to the condition that the optimal value V can be perfectly reconstructed from the representation (S, Z) .

Lemma E.1 (Characterization of Value Sufficiency). *Assume $V = v(S, G)$ and $Z = \phi_V(S, G)$ are deterministic measurable functions of (S, G) . Then the following are equivalent:*

- (i) Z is value-sufficient, i.e. $I(V; G | S, Z) = 0$.
- (ii) $V \perp G | (S, Z)$.
- (iii) V is $\sigma(S, Z)$ -measurable, i.e. there exists a measurable map \tilde{v} such that

$$V = \tilde{v}(S, Z) \quad \text{a.s.} \tag{18}$$

Proof. (i) \iff (ii). This follows immediately from the standard property of conditional mutual information: $I(X; Y | Z) = 0$ if and only if X and Y are conditionally independent given Z . Thus, $I(V; G | S, Z) = 0 \iff V \perp G | (S, Z)$.

(ii) \implies (iii). Let $f : \mathbb{R} \rightarrow \mathbb{R}$ be any bounded measurable function. By the conditional independence assumption $V \perp G | (S, Z)$, we have:

$$\mathbb{E}[f(V) | S, Z, G] = \mathbb{E}[f(V) | S, Z] \quad \text{a.s.} \tag{19}$$

However, since $V = v(S, G)$ is a deterministic function of (S, G) , V is measurable with respect to $\sigma(S, G)$. Consequently, conditioning on (S, G) (and thus (S, Z, G) since Z is determined by S, G) reveals V exactly:

$$\mathbb{E}[f(V) | S, Z, G] = f(V) \quad \text{a.s.} \tag{20}$$

Combining (19) and (20), we obtain:

$$f(V) = \mathbb{E}[f(V) | S, Z] \quad \text{a.s.}$$

Since the right-hand side is $\sigma(S, Z)$ -measurable, $f(V)$ is $\sigma(S, Z)$ -measurable for all bounded measurable f . Choosing f as the identity (or appropriate indicators) implies V is $\sigma(S, Z)$ -measurable. By the Doob–Dynkin lemma, there exists a measurable function \tilde{v} such that $V = \tilde{v}(S, Z)$ almost surely.

(iii) \Rightarrow (ii). If $V = \tilde{v}(S, Z)$ almost surely, then V is fully determined by (S, Z) . Therefore, for any measurable set B , $P(V \in B | S, Z, G) = \mathbf{1}_{\tilde{v}(S, Z) \in B} = P(V \in B | S, Z)$, which implies $V \perp G | (S, Z)$. \square

E.2. General Decomposition of Action-Relevant Information

Here, we derive the general information-theoretic decomposition that relates action-relevant goal information to any intermediate representation Z and the value signal V .

Proposition E.2 (Exact Decomposition of Action Information). *Let $V = v(S, G)$ and $Z = \phi_V(S, G)$ be deterministic measurable functions of (S, G) . Then the following identity holds:*

$$I(A; G | S, Z) = I(A; G | S, V) - I(A; Z | S, V) + I(A; V | S, Z). \quad (21)$$

Proof. We derive the decomposition using the chain rule for conditional mutual information.

First, consider the term $I(A; G, V | S, Z)$. Since V is a deterministic function of (S, G) , knowing G (given S) determines V . Thus, adding V to the target variables does not change the information:

$$I(A; G | S, Z) = I(A; G, V | S, Z).$$

Applying the chain rule to the pair (G, V) :

$$I(A; G, V | S, Z) = I(A; V | S, Z) + I(A; G | S, Z, V). \quad (22)$$

Next, we analyze the term $I(A; G | S, Z, V)$. Consider the mutual information $I(A; Z, G | S, V)$. We can expand this in two different ways using the chain rule:

Expansion 1: Condition on Z first.

$$I(A; Z, G | S, V) = I(A; Z | S, V) + I(A; G | S, V, Z). \quad (23)$$

Expansion 2: Condition on G first.

$$I(A; Z, G | S, V) = I(A; G | S, V) + I(A; Z | S, V, G).$$

Since $Z = \phi_V(S, G)$ is a deterministic function of (S, G) , given (S, V, G) , Z is constant. Thus, $I(A; Z | S, V, G) = 0$, yielding:

$$I(A; Z, G | S, V) = I(A; G | S, V). \quad (24)$$

Equating (23) and (24), we have:

$$I(A; Z | S, V) + I(A; G | S, V, Z) = I(A; G | S, V).$$

Rearranging for the term appearing in (22):

$$I(A; G | S, Z, V) = I(A; G | S, V) - I(A; Z | S, V).$$

Substituting this back into (22), we obtain the final result:

$$I(A; G | S, Z) = I(A; V | S, Z) + I(A; G | S, V) - I(A; Z | S, V).$$

\square

E.3. The Information Gap under Value Sufficiency

We now show that if a representation is value-sufficient, the decomposition simplifies, explicitly highlighting the irreducible information gap caused by value level sets.

Corollary E.3 (Decomposition under Value Sufficiency). *If Z is value-sufficient, then $I(A; V | S, Z) = 0$ and hence*

$$I(A; G | S, Z) = I(A; G | S, V) - I(A; Z | S, V). \quad (25)$$

Proof. By Lemma E.1, if Z is value-sufficient, there exists a measurable function \tilde{v} such that $V = \tilde{v}(S, Z)$ almost surely. This implies that V is fully determined by (S, Z) . Consequently, V contains no additional information about A given (S, Z) , so $I(A; V | S, Z) = 0$. Substituting this into the identity from Proposition E.2 yields the stated result. \square

F. A Sufficient Condition for $I(A; G | S, V) > 0$

In Section 5, we argued that conditioning on the optimal value V is typically insufficient to resolve goal-dependent action ambiguity, implying $I(A; G | S, V) > 0$. In this appendix, we formalize this claim by providing a purely stochastic sufficient condition based on *conditional action variance*.

F.1. Formal Setup and Assumption

Let S, G, A, V be random variables on a probability space $(\Omega, \mathcal{F}, \mathbb{P})$ taking values in measurable spaces $(\mathcal{S}, \mathcal{B}(\mathcal{S}))$, $(\mathcal{G}, \mathcal{B}(\mathcal{G}))$, $(\mathcal{A}, \mathcal{B}(\mathcal{A}))$, and $(\mathbb{R}, \mathcal{B}(\mathbb{R}))$. In this section, we use \mathbb{P} to explicitly denote the underlying probability measure, whereas the main text overloads P for (conditional) laws and distribution functions.

Assumption F.1 (Positive Conditional Action Variance). There exists a family of measurable action events

$$\{B_{s,v} \subseteq \mathcal{A} : (s, v) \in \mathcal{S} \times \mathbb{R}\}$$

such that the induced random event $\{A \in B_{S,V}\}$ satisfies:

$$\mathbb{E} \left[\text{Var}(\mathbb{P}(A \in B_{S,V} | S, V, G) | S, V) \right] > 0. \quad (26)$$

Here, each $B_{s,v} \in \mathcal{B}(\mathcal{A})$ represents an action set dependent on the state and value.

F.2. Intuition and Plausibility

Intuitive Meaning. This assumption captures the fundamental limitation of value as a scalar signal: V typically encodes “distance” or “difficulty,” but discards “direction.” Consider an agent at a fork in the road; two goals may be equidistant (same V) yet require opposite actions (different A). The assumption serves as a stochastic detector for this phenomenon, checking if the action distribution fluctuates across goals within an iso-value set. If it does, V has failed to screen off G from A .

Plausibility in Non-Trivial Environments. This condition is satisfied in almost any environment beyond simple 1D tasks.

- **Symmetry:** Spatial symmetries naturally create the “fork” scenario described above (e.g., targets N steps away in opposite directions have identical values but distinct optimal actions).
- **General Case:** In high-dimensional state spaces, value level sets are typically large manifolds that almost invariably encompass goals requiring different optimal actions, unless the value function is pathologically unique for every goal-action pair.

F.3. Lower Bound for $I(A; G | S, V)$

We now show that positive conditional action variance implies a positive information gap.

Proposition F.2 (Positive Conditional Action Variance $\Rightarrow I(A; G | S, V) > 0$). *Under Assumption F.1, the conditional mutual information is strictly positive and lower-bounded by the conditional action variance:*

$$I(A; G | S, V) \geq 2 \mathbb{E} \left[\text{Var}(\mathbb{P}(A \in B_{S,V} | S, V, G) | S, V) \right] > 0. \quad (27)$$

Proof. We utilize Pinsker’s inequality for Bernoulli distributions. For $\text{Bern}(p)$ and $\text{Bern}(q)$, Pinsker’s inequality implies:

$$\text{KL}(\text{Bern}(p) \| \text{Bern}(q)) \geq 2(p - q)^2. \quad (28)$$

Define the binary random variable indicating whether the action falls into the target set:

$$Y := \mathbf{1}\{A \in B_{S,V}\} \in \{0, 1\}.$$

Since Y is a deterministic function of (S, V, A) , the data processing inequality for conditional mutual information gives:

$$I(A; G | S, V) \geq I(Y; G | S, V). \quad (29)$$

Now, let p be the goal-dependent probability and \bar{p} be the marginalized probability (averaged over goals):

$$p := \mathbb{P}(Y = 1 \mid S, V, G) = \mathbb{P}(A \in B_{S,V} \mid S, V, G),$$

$$\bar{p} := \mathbb{P}(Y = 1 \mid S, V) = \mathbb{E}[p \mid S, V].$$

Conditioned on (S, V, G) , $Y \sim \text{Bern}(p)$, and conditioned on (S, V) alone, the marginal distribution is $Y \sim \text{Bern}(\bar{p})$. Expressing $I(Y; G \mid S, V)$ as the expected KL divergence:

$$I(Y; G \mid S, V) = \mathbb{E}[\text{KL}(\text{Bern}(p) \parallel \text{Bern}(\bar{p}))].$$

Applying Pinsker's inequality (28) pointwise:

$$I(Y; G \mid S, V) \geq \mathbb{E}[2(p - \bar{p})^2].$$

Finally, recognizing that $\mathbb{E}[(p - \bar{p})^2 \mid S, V]$ is precisely the conditional variance of p :

$$\mathbb{E}[(p - \bar{p})^2] = \mathbb{E}[\text{Var}(p \mid S, V)] = \mathbb{E}[\text{Var}(\mathbb{P}(A \in B_{S,V} \mid S, V, G) \mid S, V)].$$

Combining this with (29) yields the bound in (27). The strict positivity follows directly from Assumption F.1. \square

G. Discrete Cube: Detailed Setup

This appendix provides comprehensive details on the Discrete Cube environment introduced in Section 6, including the full specification of states, actions, transitions, the computation of optimal values and policies, the construction of the representation library, and the evaluation protocol.

G.1. Environment Specification

State space. The environment is a 4×4 grid containing an agent and two cubes (Red and Blue). A state is defined as:

$$s = (p_a, p_r, p_b, h) \in \mathcal{S},$$

where:

- $p_a = (x_a, y_a) \in \{0, 1, 2, 3\}^2$ is the agent position,
- $p_r = (x_r, y_r)$ is the red cube position (or a special ‘held’ marker when held),
- $p_b = (x_b, y_b)$ is the blue cube position (or a special ‘held’ marker when held),
- $h \in \{\text{none, red, blue}\}$ is the gripper status.

When $h = \text{red}$, the red cube moves with the agent so that $p_r = p_a$; similarly for $h = \text{blue}$. The two cubes cannot occupy the same position when both are on the floor, i.e., $p_r \neq p_b$ when $h = \text{none}$.

For $n = 4$, the state space contains 4,352 reachable states.

Action space. The action set consists of six discrete actions:

$$\mathcal{A} = \{\text{up, down, left, right, pick, place}\}.$$

Transition dynamics. Transitions are deterministic:

- **Movement actions** (up, down, left, right): Move the agent by one cell in the specified direction, clipped at grid borders. If the agent is holding a cube, the cube moves with the agent.
- **pick**: Succeeds if and only if $h = \text{none}$ and the agent is on a cube. The agent picks up the cube at its current position.
- **place**: Succeeds if and only if $h \neq \text{none}$ and the agent’s current position is not occupied by another cube. The held cube is placed at the agent’s position.

Goal space. A goal specifies a target cube and a desired position:

$$g = (t, p_g) \in \mathcal{G}, \quad t \in \{\text{red, blue}\}, p_g \in \{0, 1, 2, 3\}^2.$$

For $n = 4$, we have $|\mathcal{G}| = 2 \times 16 = 32$ goals.

Success condition. A state s is successful for goal $g = (t, p_g)$ if and only if:

1. The target cube t is at position p_g , and
2. The agent is not holding the target cube ($h \neq t$).

State-goal pair filtering. To ensure well-defined optimal actions and exclude trivial or degenerate cases, we filter the set of (s, g) pairs used for computing information-theoretic quantities:

- When $h = \text{none}$: the red cube, blue cube, and goal positions must all be mutually distinct ($p_r \neq p_b, p_r \neq p_g, p_b \neq p_g$).
- When $h \neq \text{none}$: the agent position, floor cube position, and goal position must all be mutually distinct.

After filtering, we obtain 120,960 valid (s, g) pairs for $n = 4$.

G.2. Optimal Value and Policy via BFS

Shortest-path distance. For each goal g , we compute the exact optimal distance-to-success $D^*(s, g) \in \mathbb{N}$ for all states s using breadth-first search (BFS) backward from the success states:

1. Initialize $D^*(s, g) = 0$ for all success states (where target cube is at p_g and $h \neq t$).
2. Propagate distances backward through the transition graph: for each state s' with an action a leading to state s , set $D^*(s', g) = D^*(s, g) + 1$ if not yet visited.
3. Continue until all reachable states are labeled.

Optimal value function. We define the optimal value as the negative distance:

$$V^*(s, g) := -D^*(s, g).$$

This represents the (negated) minimum number of steps required to achieve the goal from state s .

For intuition, when not holding any cube, the distance roughly satisfies:

$$D^*(s, g) \approx d_{at}(s, g) + d_{bg}(s, g) + 2,$$

where d_{at} is the Manhattan distance from agent to target cube, d_{bg} is the Manhattan distance from target cube to goal, and $+2$ accounts for `pick` and `place` actions. The exact BFS computation handles edge cases where this approximation breaks down (e.g., when holding the non-target cube).

Optimal action distribution. An action a is optimal at state s for goal g if and only if executing a leads to a successor state s' with:

$$D^*(s', g) = D^*(s, g) - 1 \quad \Leftrightarrow \quad V^*(s', g) = V^*(s, g) + 1.$$

Let $\mathcal{A}^*(s, g) \subseteq \mathcal{A}$ denote the set of optimal actions. We define the optimal action distribution with uniform tie-breaking:

$$P^*(a | s, g) = \begin{cases} \frac{1}{|\mathcal{A}^*(s, g)|} & \text{if } a \in \mathcal{A}^*(s, g), \\ 0 & \text{otherwise.} \end{cases}$$

G.3. Feature Representation

For constructing goal representations, we define the following features based on relative positions. Let (x_a, y_a) be the agent position, (x_t, y_t) the target cube position, and (x_g, y_g) the goal position.

Directional features.

$$\begin{aligned} dx_1 &= x_t - x_a, & dy_1 &= y_t - y_a, \\ dx_2 &= x_g - x_t, & dy_2 &= y_g - y_t. \end{aligned}$$

Here (dx_1, dy_1) points from the agent to the target cube, and (dx_2, dy_2) points from the target cube to the goal.

Distance features.

$$\begin{aligned} d_{at} &= |dx_1| + |dy_1|, \\ d_{bg} &= |dx_2| + |dy_2|. \end{aligned}$$

Handling held cubes. When the agent is holding the target cube, we set $(x_t, y_t) = (x_a, y_a)$ so that $dx_1 = dy_1 = 0$ and $d_{at} = 0$.

G.4. Representation Library

We construct a diverse library of goal representations $\phi : \mathcal{S} \times \mathcal{G} \rightarrow \mathcal{Z}$ to systematically explore the (Δ_V, Δ_A) space.

G.4.1. BASELINE REPRESENTATIONS

We define four baseline representations that anchor different regions of the sufficiency space:

1. **full:** $Z = (h, t, dx_1, dy_1, dx_2, dy_2)$.

Preserves complete directional information. This representation is both action-sufficient ($\Delta_A = 0$) and value-sufficient ($\Delta_V = 0$) by construction, as it retains all information needed to determine both the optimal action and the optimal value.

2. **signs:** $Z = (h, t, \text{sgn}(dx_1), \text{sgn}(dy_1), \text{sgn}(dx_2), \text{sgn}(dy_2))$.

Coarsens directions to signs only $(-1, 0, +1)$, discarding magnitude information. This representation is nearly action-sufficient ($\Delta_A \approx 0.0003$) because directional signs are typically sufficient to determine the optimal movement direction. However, it is value-insufficient ($\Delta_V \approx 0.99$) because different magnitudes correspond to different distances (and hence values).

3. **value_only:** $Z = (V^*, .)$.

Preserves only the optimal value. By construction, this is perfectly value-sufficient ($\Delta_V = 0$). However, it is highly action-insufficient ($\Delta_A \approx 0.23$) because many different state-goal pairs share the same value while requiring different optimal actions.

4. **distances:** $Z = (h, d_{at}, d_{bg})$.

Preserves distances but not directions. This is value-sufficient ($\Delta_V = 0$) since the value depends only on distances. However, it is action-insufficient ($\Delta_A \approx 0.08$) because different directions with the same distances require different movement actions.

G.4.2. RANDOM REPRESENTATION GENERATION

To broadly cover the (Δ_V, Δ_A) plane, we generate 2000 random representations using a template-based approach. Each random representation is constructed by:

1. Sampling a template type from a predefined set with specified probabilities.
2. Sampling template-specific parameters (e.g., which features to include, which transforms to apply).

Feature transforms. We define several transforms that can be applied to individual features:

Directional transforms (applied to dx_1, dy_1, dx_2, dy_2):

- `raw`: identity, $x \mapsto x$
- `sign`: sign function, $x \mapsto \text{sgn}(x) \in \{-1, 0, +1\}$
- `abs`: absolute value, $x \mapsto |x|$
- `clip_k`: clip to $[-k, k]$, i.e., $x \mapsto \max(-k, \min(k, x))$ for $k \in \{1, 2, 3\}$
- `parity`: parity of absolute value, $x \mapsto |x| \bmod 2$
- `sgn_bucket_k`: signed bucket, $x \mapsto \text{sgn}(x) \cdot \min(|x|, k)$ for $k \in \{2, 3\}$

Distance transforms (applied to d_{at}, d_{bg}):

- `raw`: identity
- `bucket_k`: $x \mapsto \min(x, k)$ for $k \in \{2, 3, 4\}$
- `parity`: $x \mapsto x \bmod 2$

Value transforms (applied to V^*):

- `raw`: identity
- `bucket_3`: bucket the cost $-V^*$ into $\{0, 1, 2, 3, \geq 4\}$

Template types. The random representations are generated from the following templates:

- `value_plus`: Includes holding status, optionally target identity, and a transformed value. Tends to be value-sufficient with varying action sufficiency.
- `dist_coarse`: Includes holding status, optionally target identity, and transformed distances d_{at}, d_{bg} . Explores the value-sufficient but action-insufficient region.
- `dir_subset`: Includes holding status, optionally target identity, and a random subset of directional signs. Explores action-sufficient but value-insufficient region.
- `dir_coarse`: Includes all four directional features with independently sampled transforms. Covers a wide range of both sufficiency measures.
- `mixed_dir_dist`: Combines a subset of directional features with distance features, each with random transforms.
- `phase_split`: Conditions representation on the gripper status (holding vs. not holding), using different feature subsets for each phase.
- `proj_mod`: Projects directional features through random linear combinations modulo a small integer.
- `two_hash`: Hashes pairs of directional features independently.
- `hashed_actor`: Hashes the full directional tuple modulo a random integer, introducing collisions that degrade both sufficiency measures.
- `hashed_dist`: Hashes the distance tuple modulo a random integer.
- `drop_id`: Drops target identity, forcing the representation to be shared across red and blue cube goals.

Templates are sampled with weights designed to cover the (Δ_V, Δ_A) plane broadly.

G.5. Mixed Policy and Control Evaluation

Mixed policy. Given a representation ϕ , the mixed policy conditions only on the current state s and the representation value $z = \phi(s, g)$:

$$\pi_\phi(a | s, z) := \mathbb{E}[P^*(a | s, G) | S = s, Z = z] = \sum_{g: \phi(s, g) = z} P^*(a | s, g) \cdot P(G = g | S = s, Z = z).$$

Under the uniform distribution over filtered (s, g) pairs, this simplifies to averaging $P^*(\cdot | s, g)$ uniformly over all goals g that map to the same z :

$$\pi_\phi(a | s, z) = \frac{1}{|\{g : \phi(s, g) = z\}|} \sum_{g: \phi(s, g) = z} P^*(a | s, g).$$

Rollout procedure. To evaluate control success, we sample tasks and execute rollouts:

1. **Task sampling:** Sample 600 tasks (s_0, g) where $h(s_0) = \text{none}$ and the target is not already at the goal.
2. **Horizon setting:** For each task, set $H = \min\{D^*(s_0, g) + 6, 30\}$, where the margin $m = 6$ and cap $H_{\max} = 30$ prevent indefinite wandering while allowing some slack for suboptimal actions.
3. **Rollout:** For each task, execute 50 independent rollouts. At each step t :
 - (a) Compute $z_t = \phi(s_t, g)$.
 - (b) Sample $a_t \sim \pi_\phi(\cdot | s_t, z_t)$.
 - (c) Execute a_t to obtain s_{t+1} .
 - (d) Terminate if success or $t \geq H$.
4. **Success rate:** For each representation ϕ , compute the fraction of rollouts that reach success.

G.6. Information-Theoretic Quantities

All information-theoretic quantities are computed exactly under the uniform distribution over filtered (s, g) pairs.

Conditional entropies.

$$\begin{aligned} H(A | S, G) &= \mathbb{E}_{s,g} \left[- \sum_a P^*(a | s, g) \log P^*(a | s, g) \right], \\ H(A | S, Z) &= \mathbb{E}_{s,g} \left[- \sum_a \pi_\phi(a | s, \phi(s, g)) \log \pi_\phi(a | s, \phi(s, g)) \right], \\ H(V | S, G) &= 0, \\ H(V | S, Z) &= \mathbb{E}_{s,g} [H(P(V | S = s, Z = \phi(s, g)))] . \end{aligned}$$

Sufficiency gaps.

$$\begin{aligned} \Delta_A &:= I(A; G | S, Z) = H(A | S, Z) - H(A | S, G), \\ \Delta_V &:= I(V; G | S, Z) = H(V | S, Z) - H(V | S, G) = H(V | S, Z). \end{aligned}$$

Within-level-set disambiguation.

$$I(A; Z | S, V) = H(A | S, V) - H(A | S, V, Z),$$

where $H(A | S, V)$ is computed by grouping (s, g) pairs by $(s, V^*(s, g))$ and averaging the entropy of the optimal action distribution within each group.

H. Proofs for Section 7

In this section, we provide the formal derivations connecting the actor training objective (log-loss) to the information-theoretic concept of action sufficiency.

H.1. Decomposition of Actor Log-Loss

We first prove that the actor's negative log-likelihood (NLL) objective is equivalent to the conditional entropy of the optimal policy plus the conditional KL risk defined in the previous sections.

Lemma H.1 (Actor Log-Loss as Excess KL Risk). *For any actor parameters (θ, ϕ) with representation $Z = \phi(S, G)$, the actor training loss satisfies:*

$$\mathcal{L}_{\text{act}}(\theta, \phi) = H(A | S, G) + \mathcal{R}(\pi_\theta, \phi), \quad (30)$$

where $\mathcal{R}(\pi_\theta, \phi)$ is the conditional KL risk.

Proof. Recall the definition of the conditional entropy of the data generating distribution:

$$H(A | S, G) = \mathbb{E}_{(S, G, A) \sim P} [-\log P(A | S, G)].$$

We expand the expression for the difference between the actor loss and the conditional entropy:

$$\begin{aligned} \mathcal{L}_{\text{act}}(\theta, \phi) - H(A | S, G) &= \mathbb{E}[-\log \pi_\theta(A | S, Z)] - \mathbb{E}[-\log P(A | S, G)] \\ &= \mathbb{E}[\log P(A | S, G) - \log \pi_\theta(A | S, Z)] \\ &= \mathbb{E}\left[\log \frac{P(A | S, G)}{\pi_\theta(A | S, Z)}\right]. \end{aligned}$$

By the law of iterated expectations, conditioning on (S, G) :

$$\begin{aligned} \mathbb{E}\left[\log \frac{P(A | S, G)}{\pi_\theta(A | S, Z)}\right] &= \mathbb{E}_{(S, G) \sim P}\left[\mathbb{E}_{A \sim P(\cdot | S, G)}\left[\log \frac{P(A | S, G)}{\pi_\theta(A | S, Z)} \mid S, G\right]\right] \\ &= \mathbb{E}_{(S, G) \sim P}\left[\text{KL}(P(\cdot | S, G) \parallel \pi_\theta(\cdot | S, Z))\right] \\ &= \mathcal{R}(\pi_\theta, \phi). \end{aligned}$$

This completes the proof. \square

H.2. Bounding the Action Sufficiency Gap

Using the decomposition derived above, we now show that minimizing the actor log-loss implicitly minimizes the irreducible information gap $I(A; G | S, Z)$.

Theorem H.2 (Near-Optimal Actor NLL Implies Approximate Action Sufficiency). *For any (θ, ϕ) with $Z = \phi(S, G)$, the action sufficiency gap is bounded by the excess loss:*

$$I(A; G | S, Z) \leq \mathcal{L}_{\text{act}}(\theta, \phi) - H(A | S, G). \quad (31)$$

Consequently, if $\mathcal{L}_{\text{act}}(\theta, \phi) \leq H(A | S, G) + \varepsilon$, then Z is ε -approximately action-sufficient.

Proof. From Lemma H.1, we have the identity:

$$\mathcal{L}_{\text{act}}(\theta, \phi) - H(A | S, G) = \mathcal{R}(\pi_\theta, \phi). \quad (32)$$

Recall the decomposition of the conditional KL risk derived in the previous section (Proposition regarding Conditional KL Risk Decomposition):

$$\mathcal{R}(\pi_\theta, \phi) = \underbrace{\mathbb{E}\left[\text{KL}(P(A | S, Z) \parallel \pi_\theta(A | S, Z))\right]}_{\text{Modeling Error} \geq 0} + \underbrace{I(A; G | S, Z)}_{\text{Representation Error}}.$$

Since the KL divergence is non-negative, the modeling error term is non-negative. Therefore:

$$\mathcal{R}(\pi_\theta, \phi) \geq I(A; G | S, Z). \quad (33)$$

Combining Eq. (32) and Eq. (33) yields:

$$I(A; G | S, Z) \leq \mathcal{R}(\pi_\theta, \phi) = \mathcal{L}_{\text{act}}(\theta, \phi) - H(A | S, G).$$

For the second part of the theorem, substituting the condition $\mathcal{L}_{\text{act}}(\theta, \phi) \leq H(A | S, G) + \varepsilon$ into the inequality gives:

$$I(A; G | S, Z) \leq (H(A | S, G) + \varepsilon) - H(A | S, G) = \varepsilon.$$

Thus, Z is ε -approximately action-sufficient. \square

I. Experimental Details

I.1. Tasks and Datasets

We evaluate our approach using the Cube environment, which is a high-dimensional robotic manipulation suite. The task requires a robotic arm to manipulate and stack cubic blocks into specific goal configurations, presenting challenges in precision and long-horizon planning. To assess the scalability of our method, we conduct experiments across three levels of task complexity based on the number of objects: `double` (2 cubes), `triple` (3 cubes), and `quadruple` (4 cubes).

For each task variation, we utilize two distinct types of datasets representing different data quality distributions. The `play` dataset is generated via an oracle planner that demonstrates near-optimal behavior and efficient paths toward objectives. In contrast, the `noisy` dataset is collected using a markovian planner with added stochasticity, resulting in sub-optimal and exploratory trajectories. The data collection process is entirely task-agnostic; agents perform random interactions by picking a cube and placing it at a random coordinate. Each resulting dataset consists of 100M transitions, structured as 100 sub-datasets containing 1,000 trajectories of 1,000 timesteps each.

I.2. Training and Evaluation Details

All offline GCRL algorithms are trained for a total of 2.5M gradient steps. We conduct intermediate evaluations every 500K steps to monitor the stability and progress of the learning process.

Success is measured against 5 specific goal configurations defined for each environment. During the evaluation phase, the agent is tested 20 times for each goal, resulting in 100 total trials per evaluation checkpoint. We report the average success rate across these trials. The specific hyperparameter configurations used for these experiments are detailed in Table 3.

Table 3. Common hyperparameters for experiments.

Hyperparameter	Value
Learning rate	3e-4
Optimizer	Adam
Minibatch size	1024
Gradient steps	2.5M
MLP size	[512, 512, 512]
Activation function	GELU
Target network update rate	0.005
Discount factor γ	0.995
Horizon reduction factor n	1 (cube-double, cube-triple), 5 (cube-quadruple)
Subgoal steps k	25
Expectile κ	0.7 (HIQL, OTA), 0.9 (GCIQL, GCIVL)
Policy extraction temperature α	3.0 (HIQL, OTA), 1.0 (GCIQL), 10.0 (GCIVL)
Goal representation dimension	10
Actor $(p_{\text{cur}}^{\mathcal{D}}, p_{\text{traj}}^{\mathcal{D}}, p_{\text{rand}}^{\mathcal{D}})$ ratio	(0, 1, 0)
Value $(p_{\text{cur}}^{\mathcal{D}}, p_{\text{traj}}^{\mathcal{D}}, p_{\text{rand}}^{\mathcal{D}})$ ratio	(0.2, 0.5, 0.3)

J. Full Results

We report full results in Table 4, including mean and standard deviation of success rates across 8 seeds.

Table 4. Success rate comparison of offline GCRL algorithms across cube tasks. Results are reported as mean \pm std and averaged across 8 seeds.

Method	Goal Rep.	cube-double		cube-triple		cube-quadruple	
		play	noisy	play	noisy	play	noisy
HIQL ^{OTA}	Value Rep. (ϕ_V)	0.26 \pm 0.10	0.25 \pm 0.02	0.16 \pm 0.03	0.09 \pm 0.03	0.01 \pm 0.01	0.02 \pm 0.01
HIQL ^{OTA}	Actor Rep. (ϕ_A)	0.42 \pm 0.03	0.29 \pm 0.03	0.41 \pm 0.04	0.19 \pm 0.04	0.28 \pm 0.05	0.08 \pm 0.02
H-Flow ^{OTA}	Value Rep. (ϕ_V)	0.26 \pm 0.04	0.28 \pm 0.04	0.15 \pm 0.03	0.10 \pm 0.01	0.01 \pm 0.01	0.01 \pm 0.01
H-Flow ^{OTA}	Actor Rep. (ϕ_A)	0.43 \pm 0.05	0.33 \pm 0.04	0.45 \pm 0.05	0.23 \pm 0.04	0.25 \pm 0.08	0.11 \pm 0.03
GCIQL	–	0.69 \pm 0.03	0.13 \pm 0.01	0.30 \pm 0.04	0.14 \pm 0.05	0.01 \pm 0.01	0.00 \pm 0.00
GCIVL	–	0.36 \pm 0.05	0.20 \pm 0.03	0.08 \pm 0.02	0.14 \pm 0.03	0.00 \pm 0.00	0.00 \pm 0.00